Rapid Intercalation of Sustainable Resource-Based Linseed Oil Fatty Amide—A Polymer Precursor in Cloisite® 93A by Microwave-Assisted Method

Ufana Riaz, Sharif Ahmad

Materials Research Laboratory, Department of Chemistry, Jamia Millia Islamia, New Delhi 110025, India

Received 6 August 2010; accepted 11 December 2010
DOI 10.1002/app.33954
Published online 16 March 2011 in Wiley Online Library (wileyonlinelibrary.com).

ABSTRACT: The present study reports a novel approach for the rapid intercalation of linseed oil-derived fatty amide (LFA) in organo-montmorillonite (OMMT)-Cloisite® 93A. The intercalation of LFA (0.25, 0.5, and 1 wt %) in Cloisite® 93A was carried by varying the microwave irradiation time from 30 to 90 s. X-ray diffraction studies confirmed that microwave irradiation resulted in higher intercalation in a shorter reaction time. The basal spacings were shifted from 12.34 to 16.45 Å on microwave irradiation for 30 s while exfoliation occurred at and beyond 60 s exposure. Controlled morphology of the nanohybrids was confirmed by transmission electron microscopy analysis on microwave irradiation for 30 s. This biomodified Cloisite® 93A could be used for the preparation of polyesters, polyesteramides, and polyurethanes of controlled morphology for various applications in biomedicine. © 2011 Wiley Periodicals, Inc. J Appl Polym Sci 121: 2317–2323, 2011

Key words: nanocomposites; irradiation; clay; microstructures; electron microscopy analysis

INTRODUCTION

Polymer nanocomposites constitute one of the most developed areas of nanotechnology. There have been extensive investigations on polymer/montmorillonite (MMT) nanocomposites due to their unique properties derived from synergetic combination of each component.[1–4] MMT has gained popularity owing to its unique properties such as high cation exchange capacity, high adsorption properties, and large surface area. Nanoscopically dispersed organically modified MMT have driven the interest of academic and industrial researchers as they lead to the enhancement of pristine polymer properties such as flame retardancy, barrier properties, ablation resistance, tensile strength modulus, and electrical conductivity.[5–11] However, intercalation of polymer/polymer precursors in MMT poses a great challenge.[12] To obtain a larger *d*-spacing, attempts have been made to modify MMT by introducing inorganic molecules such as alkyl ammonium,[13] imidazolium,[14] phosphonium,[15] and tropylium[16] through cation-exchange reaction. The surface modification of MMT is an important step in achieving polymer nanocomposites with uniform dispersion and superior performance.[17–19] Several other routes have also been employed to modify clays and clay minerals such as adsorption, ion exchange with inorganic cations and organic cations, binding of inorganic and organic anions (mainly at the edges), grafting of organic compounds, reaction with acids, pillaring by different types of poly(hydroxo metal) cations, intraparticle and interparticle polymerization, dehydroxylation and calcination, delamination and reaggregation of smectites, and lyophilisation, ultrasound, and plasma.[20]

The hazardous environmental impact of toxic chemicals have imposed stringent regulations all over the world on the use of petroleum based raw materials, which increased the demand of renewable resource derived materials.[21] Triglyceride vegetable oils have been extensively used for various applications such as coatings, inks, and agrochemicals.[21] Among several triglyceride vegetable oils, linseed oil has attracted much attention because of its abundance, relatively low cost and environmentally benign characteristics. Linseed oil contains 85% unsaturated oleic, linoleic, and linolenic fatty acids. Fatty acid derived from triglyceride vegetable oils serve as an attractive precursor for the synthesis of polymers such as polyesters, polyesteramides, polyurethanes, etc.[22] Linseed oil-based fatty amide (LFA) has been widely used as a precursor for the synthesis of such polymers.

The main objective behind the modification of the MMT is to provide hydrophobic characteristics

Correspondence to: U. Riaz (ufana2002@yahoo.co.in).
Contract grant sponsor: Department of Science and technology (DST)-Science and Engineering Research council (SERC) under ''Fast Track Scheme for Young Scientists''; contract grant number: SR/FT/CS-012/2008.

to the hydrophilic surface layer, which can permit the entry of organic polymers, besides increasing the *d*-spacing to several nanometers. To improve the properties of MMT, a fast and efficient microwave-assisted procedure was adopted for the intercalation of linseed oil fatty amide into Cloisite® 93A—a commercially available organo-MMT (OMMT). Microwave-assisted reactions are reported to have several advantages over conventional procedures in material processing, such as rapid heating to reaction temperature, enhanced reaction rates by several orders of magnitude that represent an interesting ecofriendly choice in the context of green chemistry. LFA was synthesized by microwave method using linseed oil and diethanolamine.The intercalation of LFA into MMT was carried out using different loadings of LFA (0.25, 0.5, and 1 wt %). The effect of microwave irradiation on the intercalation was investigated by varying the exposure time from 30 to 90 s. The intercalation of LFA into OMMT was confirmed by X-ray diffraction (XRD) as well as transmission electron microscopy (TEM) analyses. This facile technique of intercalation is expected to pave the path for controlled polymerization of polyurethanes and polyesters within the gallery spacing of MMT.

EXPERIMENTAL

Cloisite® 93A (Southern Clay Products, Texas, USA) was procured from Southern Clay Products. It was modified with the quaternary ammonium salt shown in Scheme 1 (M2HT = methyl, dehydrogenated ammonium tallow), with approximate composition (by mass) of 65% C18, 30% C16, and 5% C14. Linseed oil (Merck, (Mumbai, India)), diethanolamine (Merck, (Mumbai, India)), sodium methoxide (Merck, (Mumbai India)), and anhydrous sodium sulfate (Merck, (Mumbai India)) were used as received.

Synthesis of linseed oil fatty amide (LFA)

Diethanolamine (0.32 mol), sodium methoxide (0.007 mol), and linseed oil (0.1 mol) were irradiated under microwave for a period of 20 min in LG microwave oven (MW frequency: 2500 MHz; power source: 230 V, ~ 50 Hz; energy output: 800 W; input power: 1200 W). The progress of reaction was monitored by thin layer chromatography (TLC). After completion of the reaction, the product was dissolved in diethyl ether, washed with 15% aqueous NaCl solution, and dried over anhydrous sodium sulfate. Filtration of the etheral solution and removal of solvent was carried out in a rotary vacuum evaporator to obtain pure LFA resin (yield 87%).

Synthesis of Cloisite® 93A/ LFA nanohybrid

Cloisite® 93A (1.0 g) was mixed with varying amounts of LFA resin (0.25, 0.5, and 1 g). The microwave irradiation was carried out for 30, 60, and 90 s in LG microwave oven (MW frequency: 2500 MHz; power source: 230 V, ~ 50 Hz; energy output: 800 W; input power: 1200 W). The nanocomposite obtained was then washed with methanol, distilled water, again with methanol, and dried in vacuum oven at 70°C for 72 h to ensure complete removal of impurities, solvent, and water.

Characterization

XRD patterns of the nanocomposites were recorded on Philips PW 3710 powder diffractometer (Nickel filtered copper Kα radiations). For the morphological analysis, the nanocomposites were ultrasonically dispersed in water. A drop of water containing the dispersed nanocomposite was placed on a copper grid and examined under Morgagni 268-D TEM, FEI, Netherlands. ^{1}H-NMR spectrum was recorded on a JEOL GSX 300 MHz FX-1000 spectrometer using deuterated chloroform ($CDCl_3$), as a solvent, and tetramethylsilane (TMS) as an internal standard.

RESULTS AND DISCUSSION

Spectral analysis

The ^{1}H-NMR spectrum of LFA revealed the characteristic peaks as indicated in Figure 1.

^{1}H-NMR ($CDCl_3$): δ = 0.95 (—CH_3), 1.3 (—CH_2)$_4$), 1.7, 2.0, 2.4, 3.3 (—CH_2—), 3.7, 3.9 (—CH_2OH), 5.5 (OH), 5.7 (CH).

The peaks of protons in the methylene groups of the triglyceride appeared at 3.7 and 3.9 ppm. The peak at 5.7 ppm confirmed the presence of vinylic protons while the peak at 5.5 ppm corresponded to OH of CH_2. The presence of characteristic peaks of LFA in the spectrum confirmed the formation of LFA by microwave technique.[22]

XRD studies

The X-Ray diffractograms of the as-prepared Cloisite® 93A/LFA nanohybrids (Fig. 2) reveal a completely amorphous structure, which can be attributed to a number of noncrystalline impurities present in the nanohybrids that cause cluttering and hence do not reveal any information. The X-Ray diffractograms of Pristine Cloisite® 93A as well as treated Cloisite® 93A/LFA nanohybrids for different exposure times are shown in Figure 3(a–c). Pristine Cloisite® 93A [Fig. 3(a)] exhibits a diffraction peak at 3.32Å corresponding to *d* (001) basal spacing of 26.7 Å. On microwave irradiation for 30 s [Fig. 3(a)],

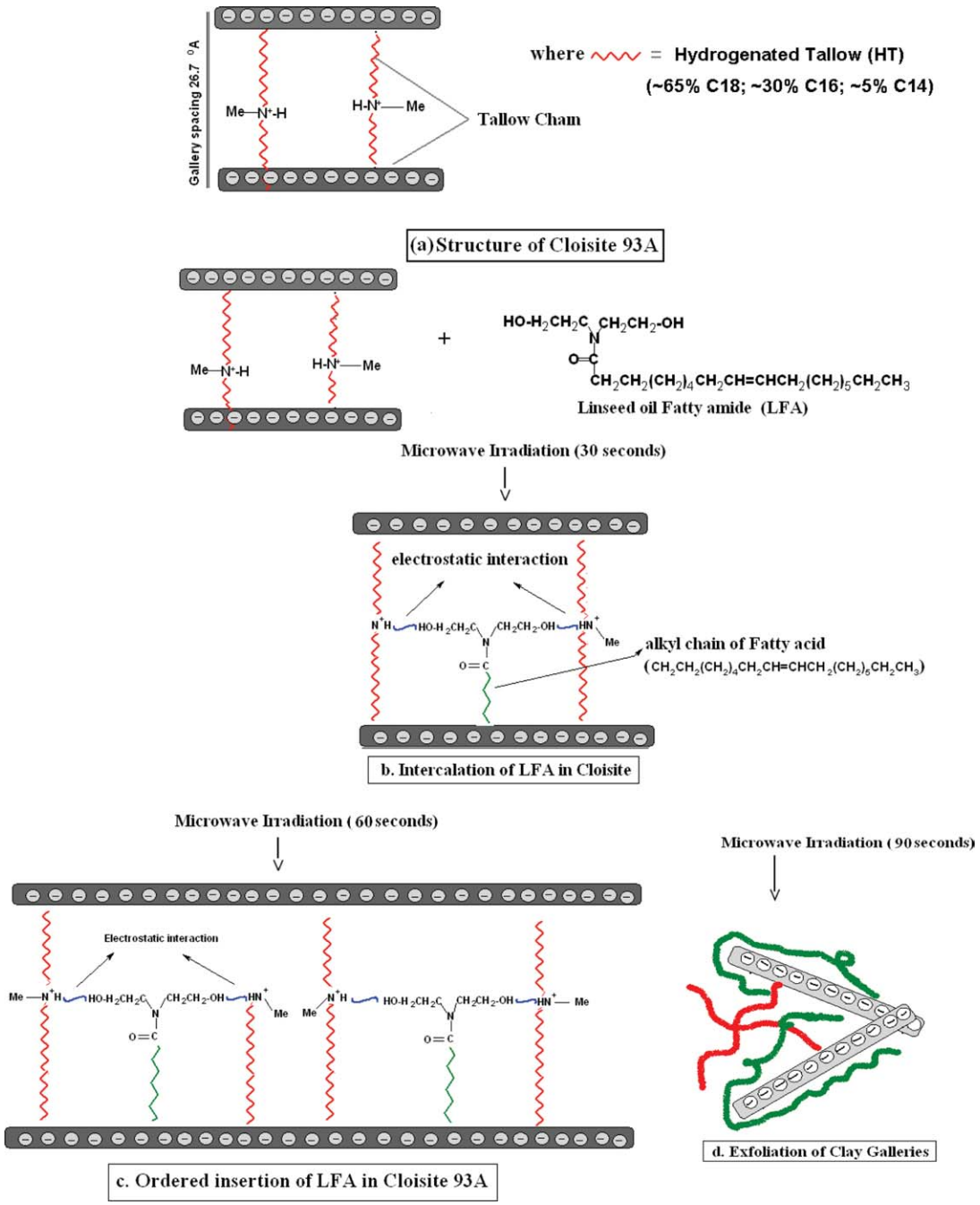

Scheme 1 Mechanism of intercalation under microwave heating. [Color figure can be viewed in the online issue, which is available at wileyonlinelibrary.com.]

the XRD pattern of Cloisite® 93A/LFA 1 : 0.25 hybrid shows a shift of about 3 Å. The small shift of basal spacing in this case can be attributed to the presence of lower LFA content (25 wt %) in Cloisite® 93A. As the loading of LFA increases to 50 wt %, the diffraction peak exhibits a characteristic shift of 4.6 Å. The shift of basal spacing on loading of LFA confirms the intercalation of LFA in Cloisite® 93A. The absence of peak broadening clearly indicates the formation of a well-ordered nanocomposite. The Cloisite® 93A /LFA 1 : 1 hybrid shows maximum intercalation as revealed by highest shifting of 6.4 Å in the *d* (001) basal spacing due to higher loading of LFA. The nanocomposite exhibits broadening as well as decrease in the intensity of the *d* (001) diffraction peak. This can be correlated to the fact that a single unit of LFA possesses two hydroxyl functional groups, which interact with the hydrogen of quaternary ammonium ion of Cloisite® 93A leading to the expansion of the basal spacing as shown in Scheme1. Under microwave irradiation, all the molecules are in highly energetic state and

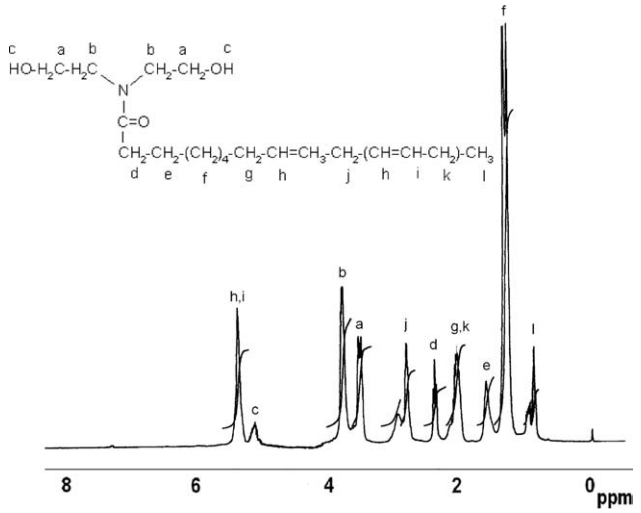

Figure 1 ^{1}H-NMR of LFA.

diffuse in the clay galleries wherein they find conducive environment to form hydrogen bond with ammonium hydrogen in the clay and make hybrid with the clay. This strong interaction acts as a driving force for the formation of self-assembled structure of LFA in Cloisite® 93A. On further increasing the exposure time to 60 s [Fig. 3(b)], the distortion of the interlayer space is confirmed by the broadening of the diffraction peaks due to the increase in the particle size of LFA. Exfoliation of the nanocomposite structure occurs when the irradiation time is increased to 90 s [Fig. 3(c)], as prolonged exposure

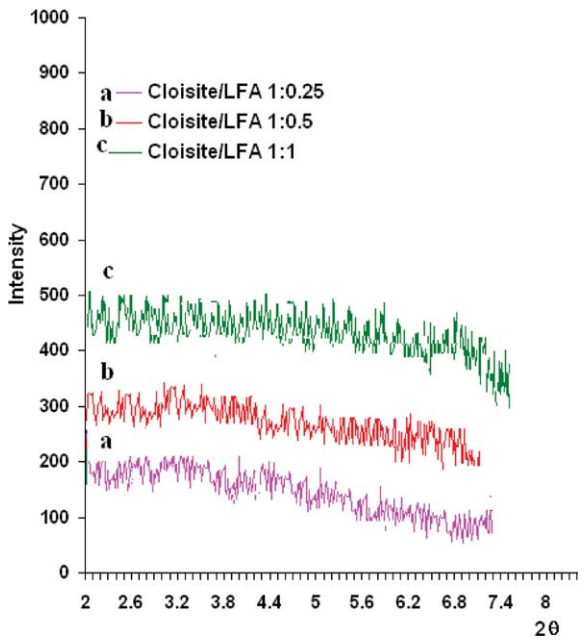

Figure 2 XRD diffractograms of as-prepared Cloisite® 93A/LFA nanohybrids. [Color figure can be viewed in the online issue, which is available at wileyonlinelibrary.com.]

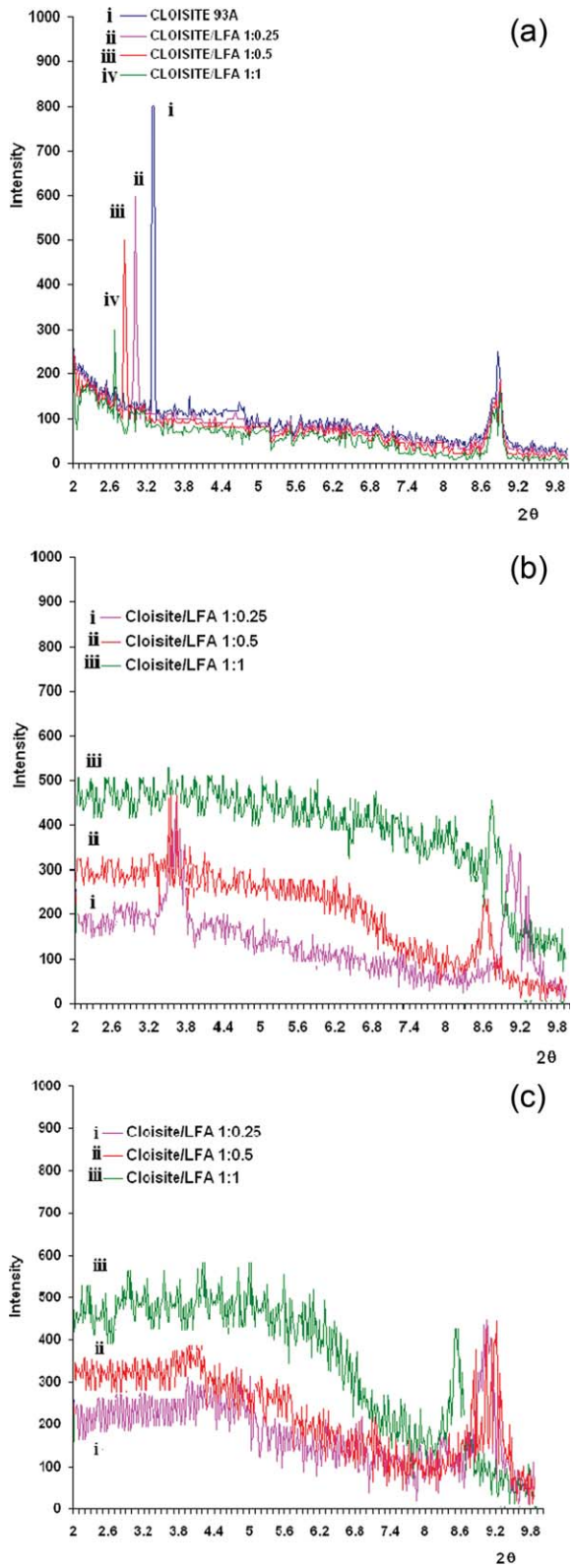

Figure 3 (a) XRD diffractograms of pristine Cloisite® 93A and treated Cloisite® 93A/LFA nanohybrids irradiated for 30 s; (b) XRD diffractograms of treated Cloisite® 93A/LFA nanohybrids irradiated for 60 s; (c) XRD diffractograms of treated Cloisite® 93A/LFA nanohybrids irradiated for 90 s. [Color figure can be viewed in the online issue, which is available at wileyonlinelibrary.com.]

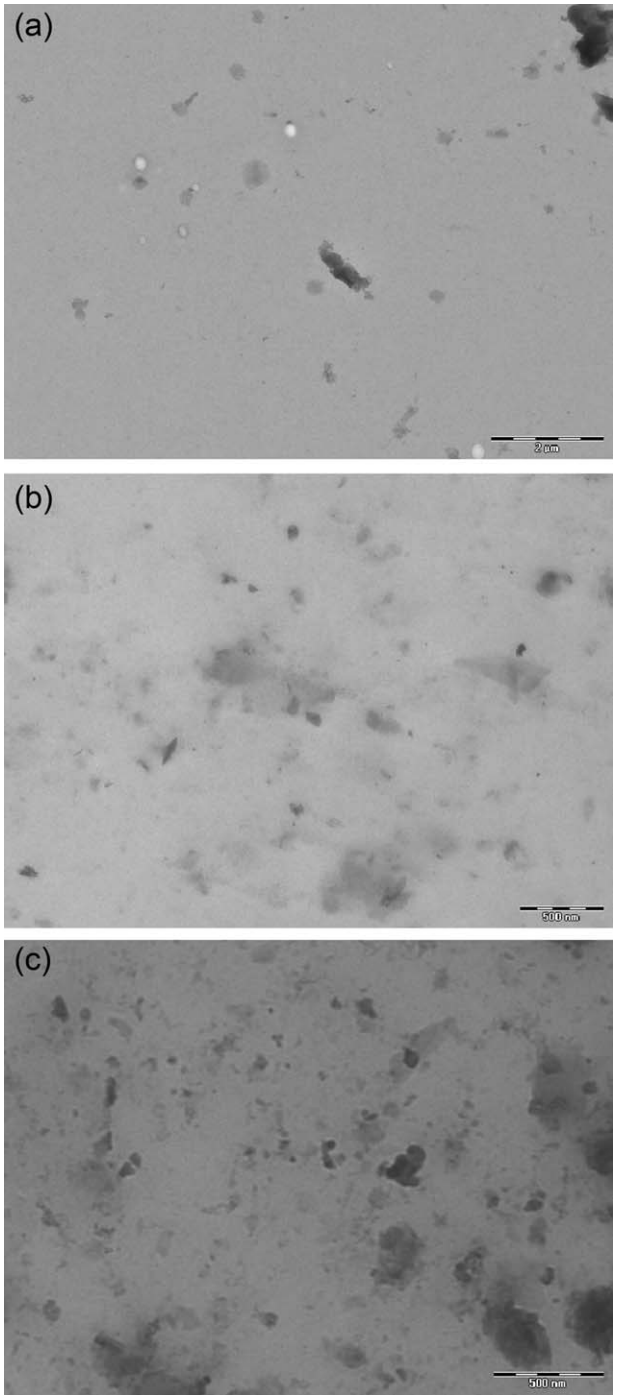

Figure 4 TEM micrographs of as-prepared (a) Cloisite® 93A/LFA 1 : 0.25, (b) Cloisite® 93A /LFA 1 : 0.5, and (c) Cloisite® 93A /LFA 1 : 1.

time leads to entanglement of the LFA chains causing disruption of the basal spacing. Scheme 1 shows the structure of Cloisite® 93A and the effect of microwave irradiation on the formation of self-assembled LFA/Cloisite® 93A nanohybrid. On microwave irradiation for 30 s, insertion of LFA chains takes place leading to an increase in the gallery height. Microwave irradiation for 60 s leads to further insertion of LFA chains forming an ordered structure. However, the microwave irradiation for 90 s leads to the disruption of the clay galleries and chain entanglement of LFA, causing exfoliation of the nanohybid.

Morphological analysis

The TEM figures of the as-prepared Cloisite® 93A / LFA nanohybrids, Figure 4(a–c) show particles of irregular shapes. The unreacted LFA and oil presumably stick to clay/LFA hybrid nanoparticles and therefore, mar the real morphology of these particles. This is apparent when we compare these TEM figures with the treated ones [Fig. 5(a–f)]. The morphology of treated Cloisite® 93A/LFA nanohybrid 1 : 0.25 irradiated for 30 s, Figure 5(a) reveals the formation of uniform self-assembly of spherical particles of an average size of 60–70 nm. With the increase in the loading of LFA [Fig. 5(b)], the particle size increases to 120 nm. Small clusters of self-assembled LFA particles are noticed. The TEM of Cloisite® 93A/LFA nanohybrid 1 : 1 [Fig. 5(c)] exhibits spherical globules of an average size of 550 nm. The homogeneous uniform morphology of this nanohybrid can be correlated to the successful intercalation of the LFA units into Cloisite® 93A. The Cloisite® 93A/LFA nanohybrid 1 : 0.25, irradiated for 60 s [Fig. 5(d)] forms tactoid-like structure while Cloisite® 93A /LFA 1 : 0 nanohybrid irradiated for the same period [Fig. 5(e)] shows an irregular dispersion of LFA particles of varying sizes. The TEM image of Cloisite® 93A/LFA nanohybrid 1 : 0.25 irradiated for 90 s [Fig. 5(f)], exhibits the formation of huge tactoids confirming exfoliation as corroborated by the XRD studies. It can be concluded that with higher loading of LFA, an increase in the interlayer space of MMT galleries takes place. Microwave irradiation for longer times (90 s) causes energetic redistribution as well as entanglement of the LFA chains, which envelope the MMT nanoparticles leading to the distortion of the well-ordered structure (Scheme 1).

CONCLUSION

The Cloisite® 93A/LFA nanohybrid synthesized via microwave-assisted intercalation formed self-assembled nanostructured composites. Microwave irradiation was found to play a crucial role in deciding the morphology as well as the intercalation of LFA in Cloisite®. Shorter exposure time and lower loading of LFA resulted in the formation of an intercalated nanocomposite while longer exposure time and higher loading of LFA distorted the uniform morphology of LFA as well as the layered structure of Cloisite® 93A, resulting in exfoliation. Further

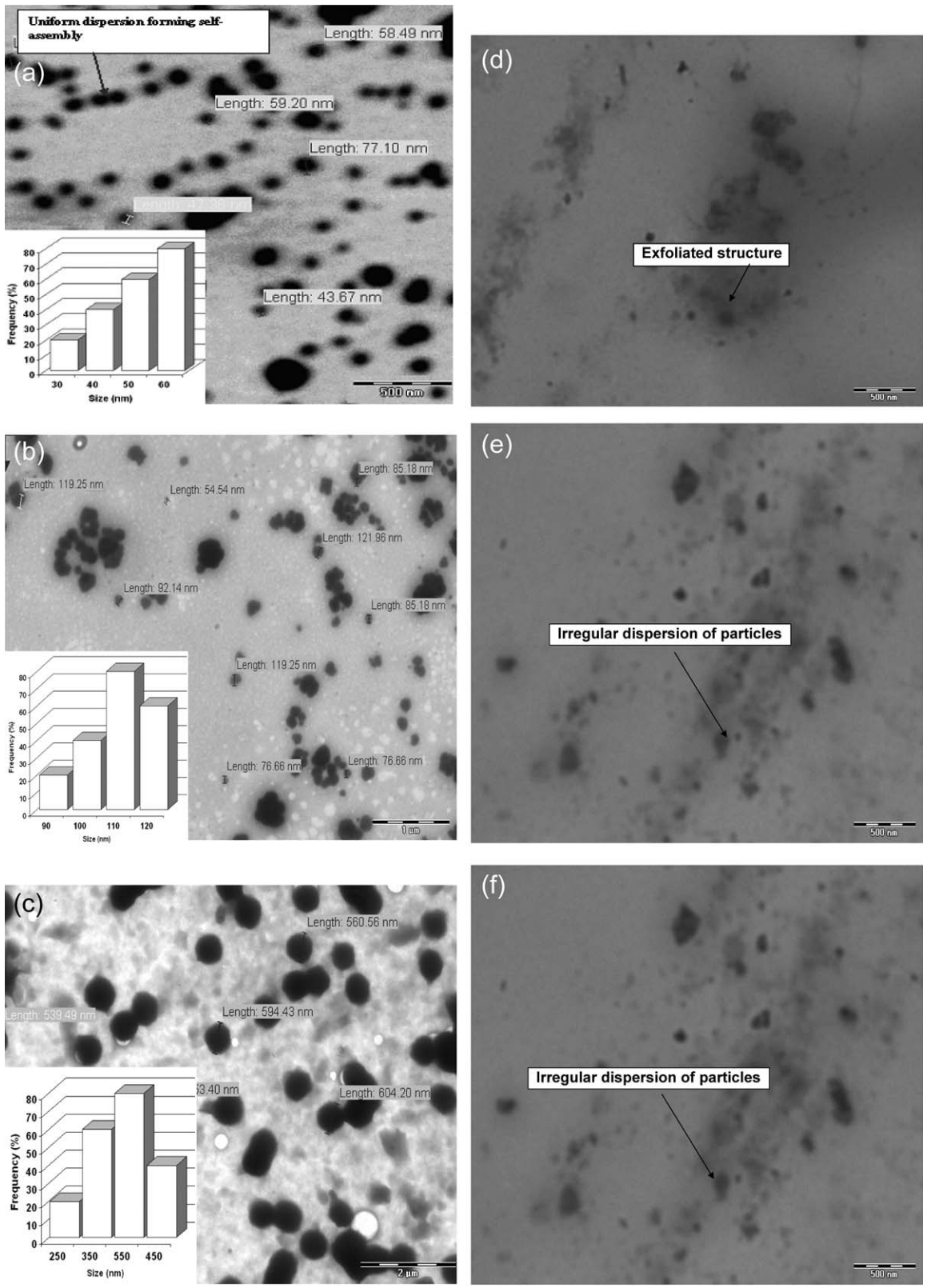

Figure 5 TEM micrographs of treated (a) Cloisite® 93A /LFA 1 : 0.25 (irradiated for 30 s), (b) Cloisite® 93A /LFA 1 : 0.5 (irradiated for 30 s), (c) Cloisite® 93A /LFA 1 : 1 (irradiated for 30 s), (d) Cloisite® 93A /LFA 1 : 0.25 (irradiated for 60 s), (e) Cloisite® 93A /LFA 1 : 0.5 (irradiated for 60 s), and (f) Cloisite® 93A /LFA 1 : 0.25 (irradiated for 90 s).

investigations on the antimicrobial and biodegradability characteristics of these bionanocomposites are underway in our laboratory and will be published soon.

The authors wish to acknowledge the Sophisticated Analytical Instrumentation Facility (SAIF) at All India Institute of Medical Sciences (AIIMS), New Delhi, India for providing the TEM facility.

References

1. Weon, J. I.; Sue, H. J. Polymer 2006, 46, 6325.
2. Joshi, S. V.; Drzal, L. T.; Mohanty, A. K.; Arora, S. Compos A 2004, 35, 371.
3. Dai, C. F.; Li, P. R.; Yeh, J. M. Eur Polym J 2008, 44, 2439.
4. Ray, S. S.; Okamoto, M. Prog Polym Sci 2003, 28, 1539.
5. Solomon, M. J.; Almusallam, A. S.; Seefeldt, K. F.; Somwangthanaroj, A.; Varadan, P. Macromolecules 2001, 34, 1864.
6. Kim, T. H.; Jang, L. W.; Lee, D. C.; Choi, H. J.; Jhon, M. S. Macromol Rapid Commun 2002, 23, 191.
7. Yeh, M. H.; Hwang, W. S.; Kuo, W. J. J Appl Phys Part 1 2005, 44, 6838.
8. Maiti, M.; Bhowmick, A. K. Polymer 2006, 47, 6156.
9. Zhang, Z.; Zhang, L.; Li, Y.; Xu, H. Polymer 2005, 46, 129.
10. Kojima, Y.; Usuki, A.; Kawasumi, M.; Okada, A.; Kurauchi, T.; Kamigaito, O. J Polym Sci Part A: Polym Chem 1993, 31, 983.
11. Litina, K.; Miriouni, A.; Gournis, D.; Karakassides, M. A.; Georgiou, N.; Klontzas, E.; Ntoukas, E.; Avgeropoulos, A. Eur Polym J 2006, 42, 2098.
12. García, S. G.; Wold, S.; Jonsson, M. Appl Clay Sci 2009, 43, 21.
13. Moraru, V. N. Appl Clay Sci 2001, 19, 11.
14. Gilman, J. W.; Award, W. H.; Davis, R. D.; Shields, J.; Harris, R. H. J.; Davis, C.; Morgan, A. B.; Sutto, T. E.; Callahan, J.; Trulove, P. C.; Delong, H. C. Chem Mater 2002, 14, 3776.
15. Zhu, J.; Morgan, A. B.; Lamelas, F. J.; Wilkie, C. A. Chem Mater 2001, 13, 3774.
16. Zhang, J.; Wilkie, C. A. Polym Degrad Stab 2004, 83, 301.
17. Scaffaro, R.; Mistretta, M. C.; Mantia, F. P. L.; Frache, A. Appl-Clay Sci 2009, 45, 185.
18. Paiva, L. B.; Morales, A. R.; Díaz, F. R. V. Appl Clay Sci 2008, 42, 8.
19. Francowski, D. J.; Capracotta, M. D.; Martin, J. D.; Khan, S. A.; Spontak, R. J. Chem Mater 2007, 19, 2757.
20. Bergaya, F.; Theng, B. K. G.; Lagaly, G. Handbook of Clay Science, 1st ed.; Amsterdam, Netherlands, Elsevier, 2006.
21. Gandini, A. Macromolecules 2008, 41, 9491.
22. Zafar, F.; Sharmin, E.; Ashraf, S. M.; Ahmad, S. J Appl Polym Sci 2005, 97, 1818.